Nitrides

DOI: 10.1002/anie.200603851

High-Pressure Synthesis of Crystalline Carbon Nitride Imide, $C_2N_2(NH)$**

Elisabeta Horvath-Bordon, Ralf Riedel, Paul F. McMillan, Peter Kroll, Gerhard Miehe, Peter A. van Aken, Andreas Zerr, Peter Hoppe, Olga Shebanova, Ian McLaren, Stefan Lauterbach, Edwin Kroke, and Reinhard Boehler*

The main-group-element nitrides Si_3N_4 and Ge_3N_4 crystallize in at least four polymorphs, including the technologically important α and β forms, a new spinel-type γ phase synthesized at high pressure and temperature, and a high-pressure δ phase.[1,2] Sn_3N_4 also forms a cubic spinel-type phase.[1,2] There is still no reliable evidence for analogous dense phases of C_3N_4. High-density C_3N_4 polymorphs were predicted to have very high bulk modulus and hardness values comparable with or exceeding that of diamond.[3–11] Many experimental studies have attempted to produce dense crystalline C_xN_y phases, by using various techniques, including high-pressure, high-temperature (HP-HT) synthesis. Solids with N:C ratios of 1.3–1.5 have been reported.[1,2] However, these materials are amorphous or nanocrystalline, and their structures and chemical compositions are not well characterized. Furthermore, the compounds prepared under HP-HT conditions are not generally recovered to ambient conditions.

Herein, we report the first synthesis of a well-crystallized compound with an N:C ratio of 3:2, in which all of the carbon atoms are tetrahedrally coordinated. Crystals of the compound are formed from the single-source precursor 1-cyanoguanidine (dicyandiamide (DCDA), $C_2N_4H_4$) under HP-HT conditions in a laser-heated diamond-anvil cell (Scheme 1). Single crystals of the new dense carbon nitride phase were recovered to ambient conditions for structural and chemical analysis.

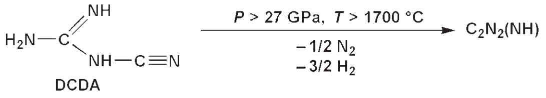

Scheme 1. Synthesis of $C_2N_2(NH)$.

The precursor was embedded in an NaCl pressure medium along with ruby chips for pressure determination. Heating was carried out with a CO_2 laser ($\lambda = 10.6$ μm), and

---

[*] Dr. E. Horvath-Bordon, Prof. Dr. R. Riedel, Dr. A. Zerr[+]
Disperse Feststoffe, Material- und Geowissenschaften
Technische Universität Darmstadt
Petersenstrasse 23, 64287 Darmstadt (Germany)
Fax: (+49) 6151-166-346
E-mail: riedel@materials.tu-darmstadt.de

Prof. Dr. P. F. McMillan, Dr. O. Shebanova
Christopher Ingold Laboratories
Department of Chemistry, University College London
20 Gordon Street, London WC1H 0AJ (UK)
and
Royal Institution of Great Britain
Davy Faraday Research, Laboratory
21 Albemarle Street, London W1S 4BS (UK)

Priv.-Doz. Dr. P. Kroll
Institut für Anorganische Chemie, RWTH Aachen
Professor-Pirlet-Strasse 1, 52056 Aachen (Germany)

Dr. G. Miehe, Dr. I. McLaren[++]
Strukturforschung, Material- und Geowissenschaften
Technische Universität Darmstadt
Petersenstrasse 23, 64287 Darmstadt (Germany)

Priv.-Doz. Dr. P. A. van Aken,[+++] Dr. S. Lauterbach
Institut für Angewandte Geowissenschaften
Material- und Geowissenschaften
Technische Universität Darmstadt
Schnittspahnstrasse 9, 64287 Darmstadt (Germany)

Dr. P. Hoppe
Abteilung Partikelchemie, Max-Planck-Institut für Chemie
55020 Mainz (Germany)

Prof. Dr. E. Kroke
Institut für Anorganische Chemie
Technische Universität Bergakademie Freiberg
09596 Freiberg (Germany)

Dr. R. Boehler
Hochdruck-Mineralphysik, Max-Planck-Institut für Chemie
55020 Mainz (Germany)

[+] Present address:
Laboratoire des Propriétés Mécaniques et Thermodynamiques des Matériaux, CNRS
Institut Galilée, Université Paris 13
99 avenue J. B. Clement, 93430 Villetaneuse (France)

[++] Present address:
Department of Physics and Astronomy
University of Glasgow, Glasgow G12 8QQ (Scotland)

[+++] Present address:
Max-Planck-Institut für Metallforschung
Heisenbergstrasse 3, 70569 Stuttgart (Germany)

[**] The work was financially supported by the Deutsche Forschungsgemeinschaft (Germany), partially in the form of a Heisenberg Fellowship (P.K.). The P.F.M. group in London is supported by the Engineering and Physical Science Research Council (UK) under Portfolio Grant EP/D504872. P.F.M. is also a Wolfson–Royal Society Research Merit Award Fellow. We thank Elmar Gröner (MPI für Chemie) for his support with the nanoSIMS, and Denis Machon (Université Claude Bernard, Lyon) and Dominik Daisenberger (University College London) for help with the diamond-anvil-cell and synchrotron experiments.

Supporting information for this article is available on the WWW under http://www.angewandte.org or from the author.

the temperature was determined by thermal emission.[12] The products were examined in situ by Raman spectroscopy. After recovery to ambient conditions, the samples were cleaned with distilled water and studied using transmission electron microscopy (TEM) techniques, including selected-area electron diffraction (SAED), electron energy-loss spectroscopy (EELS), and energy-dispersive X-ray spectroscopy (EDS). Synthesis attempts at pressures below 27 GPa and temperatures below 1700 °C yielded black amorphous products (Figure 1, part A). Treatments at higher pressures and temperatures resulted in transparent samples (Figure 1, part B).

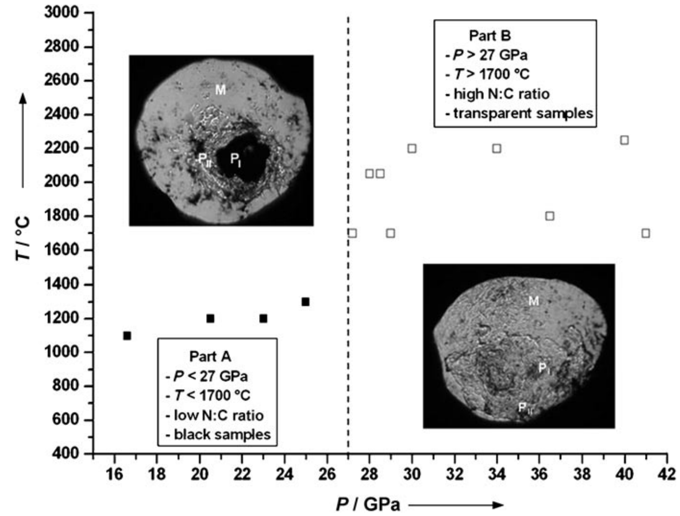

Figure 1. Pressure and temperature conditions for the synthesis of carbon nitride phases from DCDA by laser-heating. Typical optical micrographs of the products after heating at temperatures of 1100–1200 °C under pressures less than 27 GPa (part A), and after heating at temperatures of 1700–2300 °C under pressures higher than 27 GPa (part B). The diameter of the sample is 70–80 μm; P_I indicates the laser-heated part of the sample, P_{II} the cold rim of the sample, and M the pressure medium (NaCl).

Dark-field TEM images of the recovered materials revealed nanocrystals (diameters of 10–30 nm) embedded in an amorphous matrix. Extended heating (episodes of several minutes each) at temperatures higher than 1700 °C under a pressure of 41 GPa resulted in the formation of crystals of 1.0–1.5 μm in length, which were recovered to ambient conditions (Figure 2 a). No bands characteristic of C≡N bonds (ca. 2180 cm^{-1}) are visible in the Raman spectra of the products. However, broad bands at 2900–3150 cm^{-1} indicate the presence of N−H or C−H groups. Further structural characterization of the new compound excluded the presence of C−H bonds (see below). Raman spectra taken in situ at high pressure following laser-heating exhibit at least 14 bands (Figure 3). No changes were detected in the spectra during decompression to 6 GPa, before background fluorescence obscured the Raman signal.[13] The presence of hydrogen in the recovered samples was confirmed by nanoscale secondary ion mass spectrometry (nanoSIMS).[14] The H:C ratio was determined to be 0.63 ± 0.18.

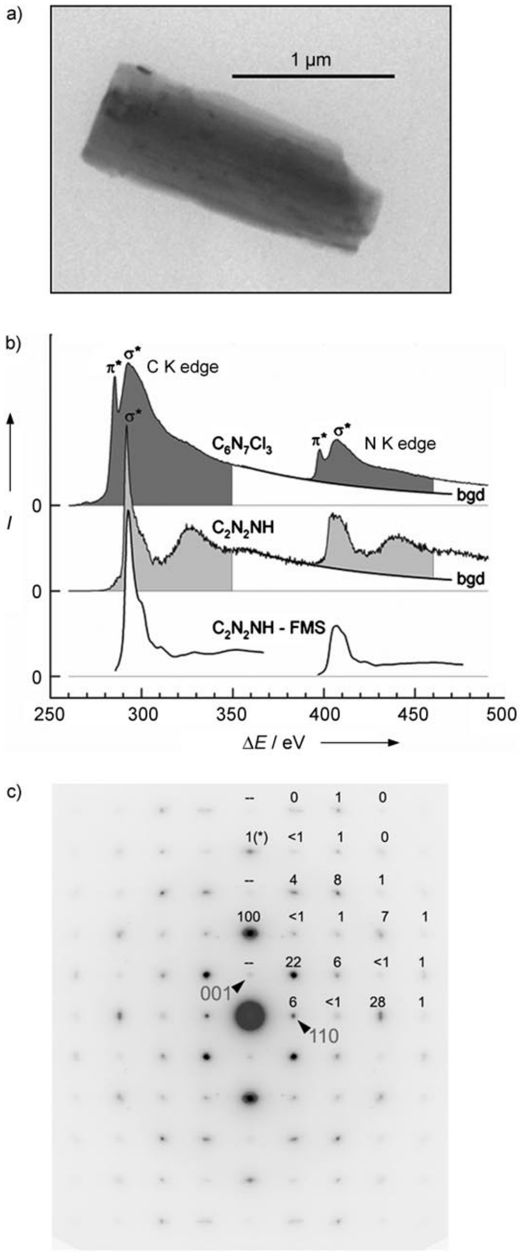

Figure 2. a) Bright-field TEM image of a crystal of $C_2N_2(NH)$ synthesized from DCDA by laser-heating at a pressure of 41 GPa and a temperature higher than 1700 °C. b) Representative C K and N K EELS edges of the reference compound $C_6N_7Cl_3$ (top) and of $C_2N_2(NH)$ (middle). The shaded areas indicate the 60-eV integration windows that start at the edge onsets. Selected orbital transitions are labeled. At the N K edges, the extrapolated power-law background is shown (bgd). The ratio of the intensity of the C K edge to that of the N K edge is 3.02 for $C_6N_7Cl_3$ and 2.18 for $C_2N_2(NH)$. The C K and N K spectra calculated for $C_2N_2(NH)$ using FMS theory are shown below the experimental spectra (see Supporting Information for details). c) SAED pattern of the $[\bar{1}10]$ zone of the orthorhombic cell of dwur-$C_2N_2(NH)$. The kinematic intensities $|F|^2$ calculated on the basis of the atomic parameters in Table 1 and scaled to 100 for reflection 002 are indicated. The intensity of reflection 400 (marked (*)) is enhanced owing to secondary diffraction from the 200 reflection.

The carbon and nitrogen contents of the recovered crystals were determined by EELS in combination with

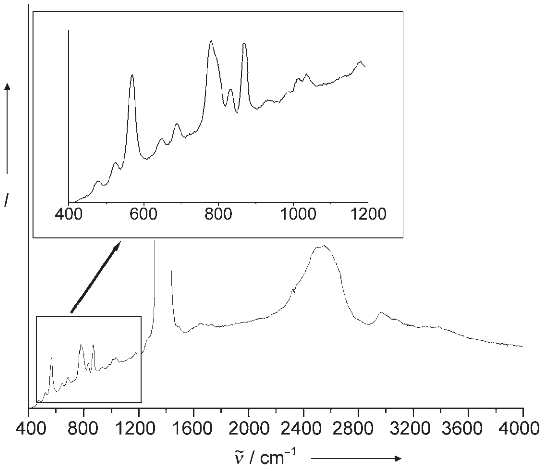

Figure 3. In situ Raman spectrum of $C_2N_2(NH)$ synthesized from DCDA by laser-heating at a pressure of 41 GPa and a temperature higher than 1700 °C. The bands between 1200 and 2700 cm^{-1} stem from the diamond-anvil cell.

theoretical calculations (Figure 2b). This technique requires the comparison of the edge intensities due to the ionization of characteristic inner-shell electrons to the partial ionization cross sections of a suitable reference compound (e.g., $C_6N_7Cl_3$). The C:N ratio was determined to be 0.62 ± 0.06.[15] No oxygen bands were detected in the EELS spectra, indicating an oxygen concentration less than 0.1–1 at %.[16] From the nanoSIMS and EELS studies, a composition of C_2N_3H ($C_2N_2(NH)$) could be derived.

The energy-loss near-edge structure (ELNES) was used to obtain information on local coordination environments (Figure 2b).[17] Pre-edge features at 285 eV at the C K edge and at 398 eV at the N K edge of $C_6N_7Cl_3$ are identified as transitions to π^* and σ^* (Figure 2) molecular orbitals (MOs), indicating trigonal-planar sp^2 bonding. In contrast, the spectra for $C_2N_2(NH)$ indicate tetrahedrally-directed sp^3 hybrid orbitals for both atoms. The first C K-edge peak at 290 eV is attributed to transitions to MOs with strong σ^* character, like those of sp^3-bonded diamond.

The crystal structure of the new compound was determined by combining electron-diffraction results with first-principles theoretical studies. The experimentally determined composition and SAED data were used first to select a set of possible crystal structures for the $C_xN_yH_z$ phase. Ab initio calculations then allowed us to refine the structure and confirm its composition. Using density functional theory (DFT),[18–22] we first examined several potential C_3N_4 structures.[4,6,23] The electron-diffraction data suggested a relationship to a hexagonal close-packed motif, as found in the lonsdaleite or wurtzite structures. Various hypothetical structures were immediately excluded on the basis of high internal energies or inherent elastic and dynamic instabilities (calculated using ab initio molecular dynamics (MD) simulations), or by their incompatibility with the observed lattice parameters and SAED intensities. Only a defect-wurtzite (dwur) structure for C_3N_4 gave good agreement with the electron-diffraction and EELS data, in particular, with respect to the coordination geometry of the nitrogen sites. In the dwur-C_3N_4 structure, the nitrogen sites are pyramidal (sp^3), rather than trigonal-planar (sp^2) as would be expected in the β- or α-C_3N_4 structures. The observed lattice spacings of the new structure are very close to a tripled ($\sqrt{3} \times \sqrt{3}$) lonsdaleite cell; however, we were unable to reconcile the dwur-C_3N_4 structure with the experimentally determined cell parameters and space group.

Once the presence of structural hydrogen atoms was recognized (by nanoSIMS) and a composition of $C_2N_2(NH)$ was determined, all of the experimental information could be integrated in a structure analogous to that adopted by $Si_2N_2(NH)$, Si_2N_2O, and a high-pressure modification of B_2O_3.[24–26] The structure of the new dwur-$C_2N_2(NH)$ phase (Figure 4) is derived from the hexagonal lonsdaleite structure and is in excellent agreement with the electron-diffraction and EELS results. With respect to the wurtzite structure, nitrogen atoms occupy one set of tetrahedral sites, and carbon atoms fill 2/3 of the tetrahedral sites of the other sublattice. The remaining sites in this sublattice are filled with hydrogen atoms bound to nitrogen. The structural parameters of dwur-$C_2N_2(NH)$ were refined using a combination of the electron-diffraction and theoretical results (Table 1). Two thirds of the nitrogen atoms (N1) in dwur-$C_2N_2(NH)$ have pyramidal coordination environments (Table 2). The dense packing of nitrogen and carbon atoms in dwur-$C_2N_2(NH)$ can be described as hexagonal close-packed. Alternatively, the $C_2N_2(NH)$, $Si_2N_2(NH)$, and Si_2N_2O structures can be described in terms of corrugated SiN or CN layers comprising Si_3N_3 or C_3N_3 six-membered rings connected by NH groups or oxygen bridges.

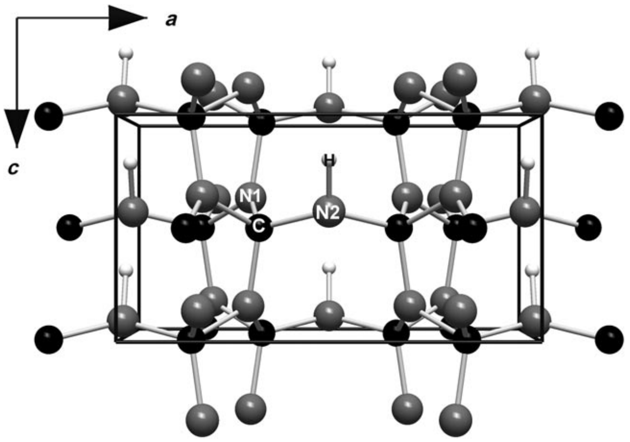

Figure 4. Defect wurtzite (dwur) structure of $C_2N_2(NH)$.

The bulk modulus calculated for dwur-$C_2N_2(NH)$ is $K_o = 277$ GPa, which is significantly lower than those of diamond and the hypothetical dense polymorphs of C_3N_4 ($K_o = 430$–460 GPa). This increased compressibility is due to the presence of N–H groups that do not contribute to the solid-state network. However, the bulk modulus of dwur-$C_2N_2(NH)$ exceeds that of β-Si_3N_4 ($K_o = 256$ GPa).[12]

The ELNES at the C K and N K edges were modeled using self-consistent full multiple scattering (FMS) theory (Figure 2b).[27] The excellent agreement between the energy

Table 1: Comparison of the structural parameters of $C_2N_2(NH)$[a] and $Si_2N_2(NH)$.[26]

Parameter	$C_2N_2(NH)$			$Si_2N_2(NH)$[26]		
Space group	*Cmc*2$_1$			*Cmc*2$_1$		
Lattice parameters						
a [Å]	7.5726			9.1930		
b [Å]	4.4425			5.4096		
c [Å]	4.0036			4.8190		
a:*b*:*c*	1.705:1:0.901			1.699:1:0.891		
Atomic positions						
Atom	*x*	*y*	*z*	*x*	*y*	*z*
C/Si	0.3295	0.3390	0	0.3263	0.3440	0
N1	0.3020	0.3651	0.3582	0.287	0.363	0.35
N2	0	0.2851	0.4240	0	0.258	0.43
H	0	0.4032	0.1956			

[a] The $C_2N_2(NH)$ structure was determined by DFT calculations. The lattice parameters determined by electron diffraction are $a = 7.536(15)$, $b = 4.434(8)$, and $c = 4.029(8)$ Å. The LDA (local density approximation) follow the usual trend for such compounds of underestimating lattice parameters by approximately 1%.

Table 2: Selected interatomic angles and distances in $C_2N_2(NH)$.

	Angle [°]		Distance [Å]
N1-C-N1	107.32 108.11 109.84	C—N1	1.45 1.46
		C—N2	1.43
N1-C-N2	113.15		
		N2—H	1.05
C-N1-C	115.70 116.19 120.37		
C-N2-C	127.78		
C-N2-H	112.12		

and intensity distributions of the calculated and observed spectra for the leading C K and N K edge maxima and for post-maximum features confirmed the structural assignment as dwur-$C_2N_2(NH)$. None of the spectra calculated for other candidate structures for C_3N_4 or $C_xN_yH_z$ compounds matched the experimental ELNES as closely.

Structural analysis was carried out by collecting SAED patterns with different zone orientations for individual single crystals of 1–1.5 μm in length. The cell parameters of $a = 7.536(15)$, $b = 4.434(8)$, $c = 4.029(8)$ Å, and $V = 139(1)$ Å^3 determined (from 7 zones) for a *C*-centered orthorhombic cell were similar to those of an equivalent hexagonal cell ($a \approx 4.4$, $c \approx 4.0$ Å). The hexagonal *c*/*a* ratio and the distribution of SAED intensities suggested a tripled wurtzite- or lonsdaleite-type structure with $\mathbf{a}' = \mathbf{a}_2 - \mathbf{a}_1$ ($a' = \sqrt{3}a$) and $\mathbf{c}' = \mathbf{c}$. In terms of such a cell, the SAED pattern in Figure 2c is of the [100] zone (equivalent to the [$\bar{1}$10] zone of the orthorhombic cell). However, in several orientations, the SAED intensities violate the hexagonal (or trigonal) symmetry. The SAED pattern of the [010] zone of the orthorhombic cell displays reflection conditions ($h0l$: $l = 2n$) consistent with space group *C*2*cm* (*Ama*2), *Cmc*2$_1$, or *Cmcm*. The structure of Si_2N_2O, in space group *Cmc*2$_1$, is the prototype for the dwur structure; $Si_2N_2(NH)$ also adopts this structure type (Table 1).[26] The reflection conditions, axial ratios, and relative intensities of the spots in the SAED pattern, as well as the chemical composition indicate that the new compound is $C_2N_2(NH)$ with a Si_2N_2O-type dwur structure.

The calculated density of dwur-$C_2N_2(NH)$ is $\rho_{calcd} = (3.21 \pm 0.3)$ g cm^{-3}, close to that of diamond ($\rho = 3.52$ g cm^{-3}). The atom density of dwur-$C_2N_2(NH)$ (172.7 atoms nm^{-3}) is very high. The cubic diamond and hexagonal lonsdaleite polymorphs of carbon have the highest atomic density of any material (176.5 atoms nm^{-3}). The atomic densities of the cubic zinc-blende-type and hexagonal wurtzite-type BN structures are slightly lower (169.3 and 167.5 atoms nm^{-3}, respectively).

If all of the interatomic interactions involved covalent bonding, dwur-$C_2N_2(NH)$ would have a low compressibility and a very high hardness. The bulk modulus K_o is related to the cohesive (binding) energy E_c and the molar volume V_m by $K_o = c\,E_c/V_m$, where $c \approx 2$–4.[28] The hardness of sp^3-bonded materials correlates well with K_o.[12] The compressibility of dwur-$C_2N_2(NH)$ is increased because of the presence of hydrogen atoms that do not contribute to cross-linking in the structure. However, the available N—H groups could undergo further condensation reactions leading to dense C_3N_4 polymorphs.

The DCDA precursor used in our HP-HT experiments was chosen as a source for a C_xN_y compound with alternating C—N units and an N:C ratio of greater than 4:3. We supposed that condensation into C_3N_4 would occur by elimination of 4/3 equivalents of NH_3 (or $1/2\,N_2 + 3/2\,H_2$). Under our reaction conditions, only 1 equivalent of NH_3 was eliminated to give $C_2N_2(NH)$ (Scheme 1).

In conclusion, we laser-heated DCDA in a diamond-anvil cell at temperatures higher than 1700 °C under pressures higher than 27 GPa and obtained a novel carbon nitride phase with an N:C ratio of 3:2. Single crystals ($\rho_{calcd} = (3.21 \pm 0.3)$ g cm^{-3}) of the product were recovered to ambient conditions. Quantitative nanoSIMS analysis revealed the presence of hydrogen, and a composition of $C_2N_2(NH)$ was determined. The new compound crystallizes in a dwur structure analogous to that of $Si_2N_2(NH)$.

Received: September 19, 2006
Revised: October 24, 2006

Keywords: carbon · density functional calculations · high-pressure chemistry · nitrides · structure elucidation

---

[1] E. Horvath-Bordon, R. Riedel, A. Zerr, P. F. McMillan, G. Auffermann, Y. Prots, W. Bronger, R. Kniep, P. Kroll, *Chem. Soc. Rev.* **2006**, *35*, 987.
[2] E. Kroke, M. Schwarz, *Coord. Chem. Rev.* **2004**, *248*, 493.
[3] M. L. Cohen, *Phys. Rev. B* **1985**, *32*, 7988.
[4] A. Y. Liu, M. L. Cohen, *Science* **1989**, *245*, 841.
[5] A. Y. Liu, M. L. Cohen, *Phys. Rev. B* **1990**, *41*, 10727.

[6] D. M. Teter, R. J. Hemley, *Science* **1996**, *271*, 53.
[7] A. Y. Liu, R. M. Wentzcovitch, *Phys. Rev. B* **1994**, *50*, 10362.
[8] Y. J. Guo, W. A. Goddard, *Chem. Phys. Lett.* **1995**, *237*, 72.
[9] P. Kroll, *J. Solid State Chem.* **2003**, *176*, 530.
[10] S. Muhl, J. M. Mendez, *Diamond Relat. Mater.* **1999**, *8*, 1809.
[11] T. Malkow, *Mater. Sci. Eng. A* **2001**, *302*, 309.
[12] R. Riedel, *Handbook of Ceramic Hard Materials*, Wiley-VCH, Weinheim, **2000**.
[13] E. D. Miller, D. C. Nesting, J. V. Badding, *Chem. Mater.* **1997**, *9*, 18.
[14] A. Benninghoven, F. G. Rüdenauer, H. W. Werner, *Secondary Ion Mass Spectrometry: Basic Concepts, Instrumental Aspects, Applications, and Trends*, Wiley, New York, **1987**.
[15] R. F. Egerton, *Electron Energy-Loss Spectroscopy in the Electron Microscope*, 2nd ed., Plenum, New York, **1996**.
[16] R. Leapman, *EELS Quantitative Analysis*, Wiley-VCH, Weinheim, **2004**.
[17] L. A. J. Garvie, A. J. Craven, R. Brydson, *Am. Mineral.* **1994**, *79*, 411.
[18] P. Hohenberg, W. Kohn, *Phys. Rev. B* **1964**, *136*, B864.
[19] W. Kohn, L. J. Sham, *Phys. Rev.* **1965**, *140*, 1133.
[20] G. Kresse, J. Hafner, *Phys. Rev. B* **1993**, *47*, 558.
[21] G. Kresse, J. Hafner, *Phys. Rev. B* **1994**, *49*, 14251.
[22] G. Kresse, J. Furthmüller, *Phys. Rev. B* **1996**, *54*, 11169.
[23] E. Kroke, M. Schwarz, E. Horath-Bordon, P. Kroll, B. Noll, A. D. Norman, *New J. Chem.* **2002**, *26*, 508.
[24] J. Sjoberg, G. Helgesson, I. Idrestedt, *Acta Crystallogr. Sect. C* **1991**, *47*, 2438.
[25] C. T. Prewitt, R. D. Shannon, *Acta Crystallogr. Sect. B* **1968**, *24*, 869.
[26] D. Peters, H. Jacobs, *J. Less-Common Met.* **1989**, *146*, 241.
[27] A. L. Ankudinov, B. Ravel, J. J. Rehr, S. D. Conradson, *Phys. Rev. B* **1998**, *58*, 7565.
[28] V. V. Brazhkin, A. G. Lyapin, R. J. Hemley, *Philos. Mag. A* **2002**, *82*, 231.